Applied Surface Science 312 (2014) 157–161

Contents lists available at ScienceDirect

Applied Surface Science

journal homepage: www.elsevier.com/locate/apsusc

Simulation study of interface traps and bulk traps in n^{++}GaN/InAlN/AlN/GaN high electron mobility transistors

M. Molnár[a,*], D. Donoval[a], J. Kuzmík[b], J. Marek[a], A. Chvála[a], P. Príbytný[a], M. Mikolášek[a], K. Rendek[a], V. Palankovski[b,c]

[a] Institute of Electronics and Photonics, Slovak University of Technology, Ilkovičova 3, 812 19 Bratislava, Slovakia
[b] Institute of Electrical Engineering, Slovak Academy of Sciences, Dúbravská cesta 9, 841 04 Bratislava, Slovakia
[c] Institute for Microelectronics, Technische Universität Wien, Guβhausstraβe 27-29, 1040 Wien, Austria

ARTICLE INFO

Article history:
Received 30 January 2014
Received in revised form 10 April 2014
Accepted 10 April 2014
Available online 21 April 2014

Keywords:
HEMT
GaN
Simulation
Modeling
Interface
Traps

ABSTRACT

We investigate the impact of interface traps and bulk traps on the performance of n^{++}GaN/InAlN/AlN/GaN high electron mobility transistors (HEMTs) using two-dimensional Sentaurus TCAD simulation. The device uses lattice-matched wide bandgap $In_{0.17}Al_{0.83}N$ as a thin barrier layer. The simulations are performed using the thermodynamic transport model. Interface and bulk traps are accounted for in our simulations. The results indicate a significant influence of both acceptor and donor traps on device operation, as long as the traps are considered in the barrier layer. On the other hand, simulations with donor traps specified at the $In_{0.17}Al_{0.83}N$/n^{++}GaN cap interface show no influence on the transfer characteristic.

1. Introduction

InAlN/GaN high electron mobility transistors (HEMTs) with lattice-matched InAlN barrier layer show higher polarization charge in the quantum well in comparison with more conventional AlGaN/GaN HEMTs. Consequently, InAlN/GaN HEMTs are less vulnerable to relaxation-related degradation mechanisms and also this system can be easily scaled down to deep submicron gate-length devices. Due to mentioned properties, they became a good alternative of conventionally used AlGaN/GaN HEMTs in a wide range of RF and power applications [1]. While substantial progress has been made in InAlN/GaN HEMTs, only a few publications [2–4] are available to explain or describe the influence of deep-level traps in these structures. To bring an understanding of deep-level traps behavior, we investigate the impact of the interface traps and bulk traps on n^{++}GaN/InAlN/AlN/GaN HEMT performance using two-dimensional Sentaurus TCAD simulation employing the thermodynamic transport model [5]. Since EHEMTs (enhancement-mode HEMTs) are becoming very popular especially for RF applications and logic circuits [6], the structure proposed by Kuzmík et al. [7] was chosen as a subject of our investigation. Traps specifications are adopted from a recent work of Sasikumar et al. [4].

2. Device structure

The device under investigation is normally off HEMT, which consists of a 2-μm GaN buffer, 1-nm AlN, 1-nm lattice-matched $In_{0.17}Al_{0.83}N$ barrier, and a 6-nm-thick GaN cap. The cap doping density is $\sim 2 \times 10^{20}$ cm^{-3}, the source-to-gate distance is 1 μm, the source-to-drain distance is 4 μm, and the gate length is 0.25 μm (Fig. 1). The gate recess through the GaN cap down to the InAlN barrier, as well as only 2-nm thick barrier layer, secures a positive threshold voltage ~0.25 V.

For the normally off operation, it is reasonable to propose the channel-to-gate separation 2-nm, consisting of a 1-nm InAlN barrier and a 1-nm AlN spacer to enhance the quantum well electron mobility [7]. There is no direct contact between the gate and the cap layer in our simulation structure and also in case of experimental devices. The resist for etching the GaN cap under the gate electrode is undercut. Together with assumed partial isotropic etching of GaN because of the low self-induced bias it ensures the separation between the gate and n^{++} GaN cap. Investigated structure and experiment is described in detail in Ref. [7]. The gap between

* Corresponding author. Tel.: +421 2 602 91 327.
E-mail address: marian.molnar@stuba.sk (M. Molnár).

http://dx.doi.org/10.1016/j.apsusc.2014.04.078
0169-4332/

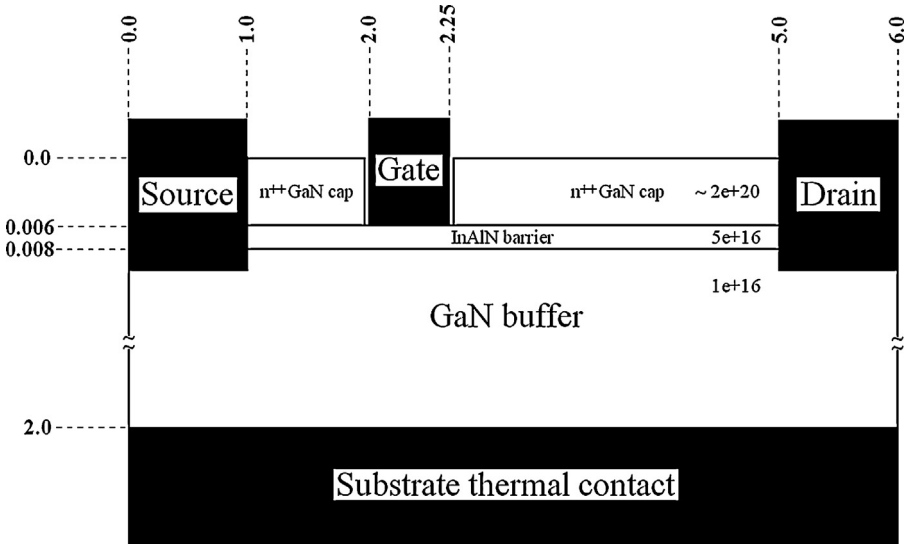

Fig. 1. Schematic view of the investigated EHEMT structure. The device dimensions are given in microns.

the gate and n^{++} GaN cap seems to be in order of a few tens of nanometers according to AFM measurement. The thickness and the doping of the GaN cap influence the HEMT direct current and microwave performance. Individual layers exhibit high n-type doping concentrations also shown in Fig. 1. These values used in our simulations are harmful and may indeed generate considerable HEMT off-state leakage, taking into account 2 micrometers thick buffer. Usually, additional p-type doping (Fe-doping or C-doing) are used to compensate unintentional n-type doping. Schottky contact barrier height ~1.4 eV is assumed in our simulations [8]. More details about the device fabrication process and performance are reported in [7,8].

3. Physics-based modeling

Two-dimensional numerical simulations are performed employing Sentaurus Device tool from Synopsys. Due to the divergence of the polarization fields at the InAlN/GaN heterointerface, a two-dimensional electron gas (2DEG) is formed in the quantum well. The sum of negative polarization charges at the InAlN/AlN interface and positive polarization charges at the AlN/GaN interface equals the polarization charges of the InAlN/GaN heterostructure without an interlayer [9]. Thus for simplification, in the model the AlN/InAlN barrier system is represented by a 2 nm thick InAlN. The polarization charges at the InAlN/GaN heterointerface and InAlN/n^{++}GaN interface are modeled as fixed interface charges with values $\sigma_{InAlN/GaN} = 2.7 \times 10^{13}\,cm^{-2}$ and $\sigma_{InAlN/n^{++}GaN} = -2.7 \times 10^{13}\,cm^{-2}$, respectively. This value, which nicely coincides with calculations and also depends on the In content in the InAlN layer, gives the best agreement with the measured data (Fig. 2). The values of used fixed charges coming from our own calculations and measurements. Relevant analytical equations and material parameters were taken from [10]. Performing thermodynamic simulations taking into account self-heating (SH), we introduce a substrate thermal contact at the bottom of the structure (Fig. 1). We obtain the best agreement with experimental data (Fig. 2) by using thermal contact resistance $R_{th} = 10^{-3}\,K\,cm^2/W$. This value lumps the thermal resistance of the nucleation layer and the substrate, and possible three-dimensional thermal effects [11]. Fig. 3 shows a family of simulated output characteristics with and without SH effect taken into account, for V_{GS} sweep from 0 V to 2.5 V with a step of 0.5 V. It is obvious that the drain current is not zero at $V_{DS} = 0$ V. This can be observed in simulations of EHEMT structures, when the drain voltage is

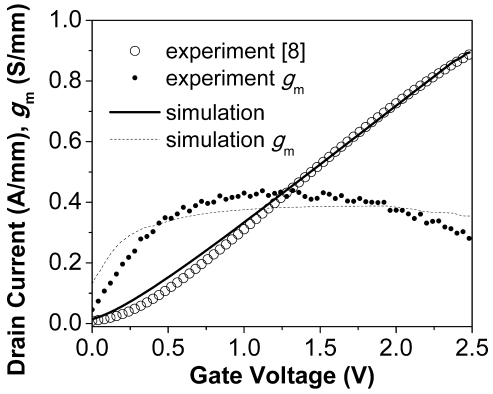

Fig. 2. Comparison of the measured and simulated transfer characteristics and transconductances of the EHEMT at $V_{DS} = 8$ V.

lower than gate voltage bias (drain current has a negative sign). By increasing the drain bias sufficiently, the gate contact becomes biased in the reverse direction. Figs. 4–5 show the energy band alignment of the investigated structure for different V_{GS} and V_{DS}, respectively. Only discrete traps were taken into account in our simulations. Figs. 4–5 also show that position of E_F for regions between the source-gate, and the gate-drain (areas with n^{++} GaN cap) is only negligible modified and therefore if we consider

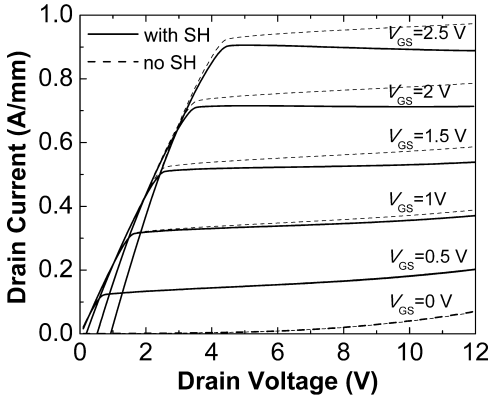

Fig. 3. Family of simulated output characteristics of EHEMT with the self-heating (SH) effect (solid line) and without SH (dashed line).

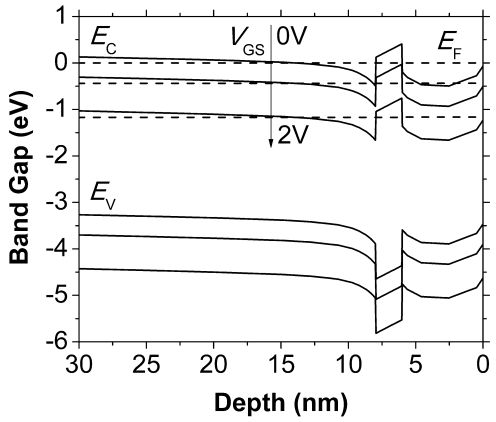

Fig. 4. Energy band alignment at V_{DS} = 8 V for different V_{GS}. The cut is done in the middle between the source and gate contacts.

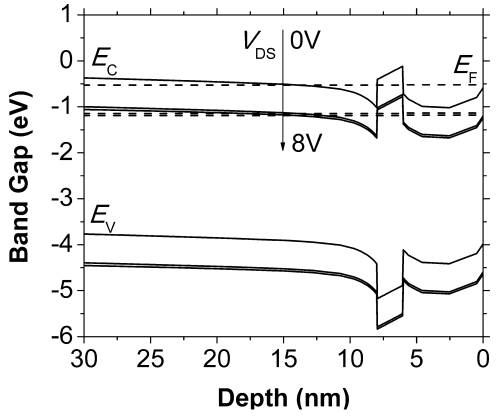

Fig. 5. Energy band alignment at V_{GS} = 2 V for different V_{DS}. The cut is done in the middle between the source and the gate contacts.

discrete traps, continuously distributed traps [12] or Gaussian distribution of traps in the energy gap, the results are the same performing the DC simulation. To our opinion using discrete traps is sufficient, to describe the role of traps qualitatively. Fig. 6 shows energy band alignment at V_{DS} = 8 V for different V_{GS}. The cut is done under the gate contact.

In our simulations the following boundary conditions are assumed. In the case of ohmic contact, we assume the charge balance at the interface. At the interface without contact, the screening

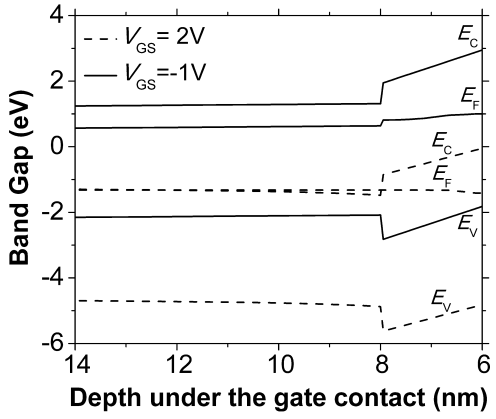

Fig. 6. Energy band alignment at V_{DS} = 8 V for different V_{GS}. The cut is done under the gate contact.

Table 1
Values of parameters for GaN and InAlN used in the simulations.

Parameter	GaN	$In_{0.17}Al_{0.83}N$
Permittivity	9.5	11.7
Band gap (eV)	3.4	4.7
Conduction band offset (eV)	0.57	–
Valence band offset (eV)	0.73	–
Electron mobility ($cm^2\,V^{-1}\,s^{-1}$)	940	1540
Hole mobility ($cm^2\,V^{-1}\,s^{-1}$)	22	82
v_{sat} for electrons ($10^7\,cm\,s^{-1}$)	2.7	4.5
β	1.7	2

method (ideal Neumann condition) is used. The thermal contact is characterized by the value of thermal resistance [5].

The thermodynamic transport model solves the Poisson equation and continuity equation as follows:

$$\nabla\varepsilon\nabla\varphi = -q(p - n + N_D - N_A) - \rho_{\text{trap}} \tag{1}$$

$$J_n = -nq\mu_n(\nabla\Phi_n + P_n\nabla T) \tag{2}$$

where ε is the electrical permittivity, φ is the electrostatic potential, q is the electronic charge, n and p are electron and hole densities, N_D is the concentration of ionized donors, N_A is the concentration of ionized acceptors and ρ_{trap} is the charge density contributed by traps and fixed charges, Φ_n is the Fermi quasi potential, P_n is the absolute thermoelectric power, and T is the lattice temperature. The doping and field dependent mobility models were used in our simulations. The doping-dependent mobility is modeled after Arora [5]:

$$\mu_{n,\text{dop}} = \mu_{\min} + \frac{\mu_d}{1 + ((N_{A,0} + N_{D,0})/N_0)^{A*}} \tag{3}$$

$$\mu_{\min} = A_{\min}\left(\frac{T}{300\ \text{K}}\right)^{\alpha m} \quad \mu_d = A_d\left(\frac{T}{300\ \text{K}}\right)^{\alpha d} \tag{4}$$

$$N_0 = A_N\left(\frac{T}{300\,\text{K}}\right)^{\alpha N} \quad A* = A_a\left(\frac{T}{300\,\text{K}}\right)^{\alpha a} \tag{5}$$

where $\mu_{\min}$, μ_d, N_0, and A^* are temperature dependent coefficients taken from [5]. The high-field mobility is modeled as follows:

$$\mu(E) = \frac{\mu_{\text{low}}E}{[1 + ((\mu_{\text{low}}E)/(v_{\text{sat}}))^{\beta}]^{1/\beta}} \tag{6}$$

Recombination through deep defect levels in the band gap is accounted for in the Shockley–Read–Hall (SRH) recombination model:

$$R_{\text{SRH}} = \frac{np - n_{ie}^2}{\tau_p(n + n_1) + \tau_n(p + p_1)} \tag{7}$$

where n_{ie} is the effective intrinsic density, and τ_n and τ_p denote the temperature-dependent lifetimes of electrons and holes, respectively. Additional auxiliary concentrations n_1 and p_1 coming from the deep levels are modeled by:

$$n_1 = n_{ie}e^{\frac{E_{\text{trap}}}{kT}} \quad p_1 = p_{ie}e^{\frac{-E_{\text{trap}}}{kT}} \tag{8}$$

where E_{trap} is the difference between the defect level and intrinsic level. Additional information about the models and parameters is described in [5]. The physical properties and values of the model parameters of GaN and $In_{0.17}Al_{0.83}N$ used in our simulations are summarized in Table 1. The table shows the maximum possible value of mobility, which is influenced by concentration of impurities and by lattice temperature.

4. Simulation results

In our simulations acceptor traps are considered with various trap concentrations at the InAlN barrier/n^{++} GaN cap interface. Fig. 7

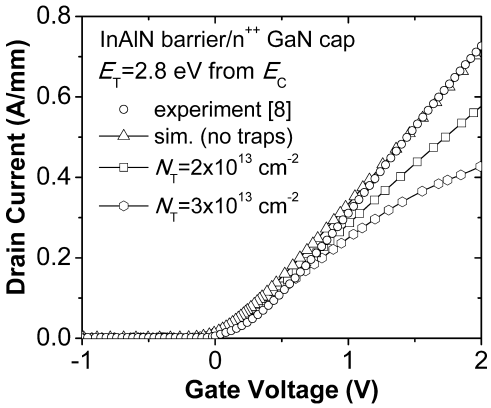

Fig. 7. The influence of acceptor traps at the InAlN barrier/GaN cap interface on the transfer characteristics at V_{DS} = 8 V. Traps energy level is specified at 2.8 eV from the conduction band of InAlN.

shows that increasing concentration of interface traps causes a drain current decrease. Unfortunately, there are no literature data on the acceptor trap levels at the InAlN/GaN interface. Assumed value is based on the known value for bulk GaN. On the other hand, simulations with donor traps specified at this interface show no influence on the transfer characteristic (not shown). In the DC (steady-state) simulation, acceptor traps are ionized only in the energy levels under the Fermi level (E_F) and donor traps are ionized only above E_F. The n^{++} GaN cap layer is degenerated (high n-type doping) and position of E_F is above E_C (Figs. 4–5). This implies that consideration of donor traps is unnecessary. In case of our study, the donor traps get ionized only for highly negative gate bias (not shown), when the E_F reaches position under the donor traps level. Next, Fig. 8 shows the influence of donor traps located in the InAlN barrier using various trap concentrations. Trap energy level $E_T = E_C - 0.6$ eV is used in our simulations. A drain current increase as well as a shift of the threshold voltage to more negative value is observed. Fig. 9 shows the free carrier concentration profiles in the n^{++} GaN/InAlN/GaN structure for different concentrations of acceptor traps in the barrier layer. We adopted the position of $E_T = E_V + 1$ eV which, as well as the capture cross-sections of $\sigma_n = 3 \times 10^{-15}$ cm^2, was identified using constant drain-current deep level transient spectroscopy (CI_D-DLTS) [4]. As Fig. 9 shows, the presence of acceptor traps influences the concentration of free carriers in the channel. The vertical cut is done in the middle between the source and gate contacts. Fig. 10 shows the influence of acceptor traps located in the InAlN barrier on the transfer characteristics. Rapid decreases of the drain current and of off-state current with increasing acceptor trap concentration

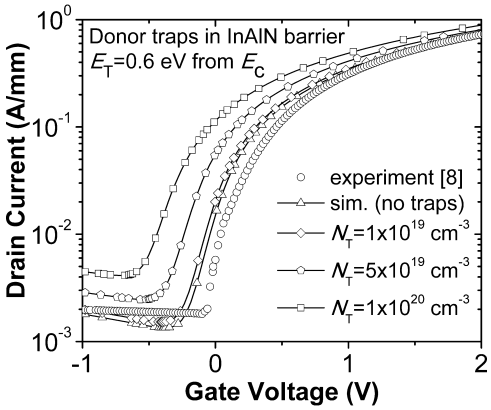

Fig. 8. The influence of donor traps in the InAlN barrier layer on the transfer characteristics at V_{DS} = 8 V. Trap energy level is specified at 0.6 eV from the conduction band of InAlN.

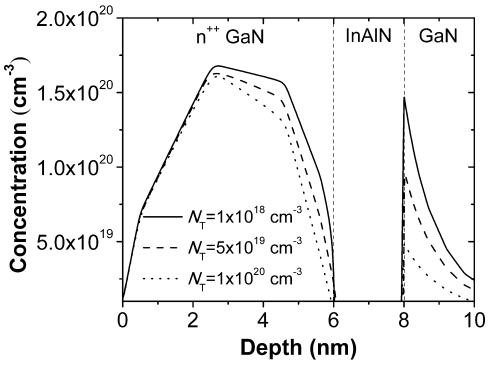

Fig. 9. Simulated free carrier concentration profile in the n^{++} GaN/InAlN/GaN structure for different concentrations of acceptor traps in the barrier layer. The vertical cut is done in the middle between the source and gate contacts.

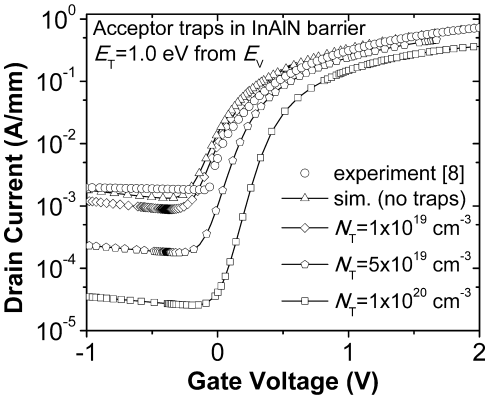

Fig. 10. The influence of acceptor traps in the InAlN barrier layer on the transfer characteristics at V_{DS} = 8 V. Traps energy level is specified at 1 eV from the valence band of InAlN [4].

are observed. Comparison of the calculated characteristics with experimental data [7,8] indicates that the reported InAlN layer was grown with concentration of traps, which does not significantly influence the dc performance of the HEMTs. This result is in agreement with the concentration of InAlN acceptor traps of only about 1.6×10^{10} cm^{-2} reported elsewhere [4].

5. Conclusion

Two-dimensional numerical device simulations employing Sentaurus Device were used to study the influence of interface traps and barrier traps in the n^{++}GaN/InAlN/AlN/GaN HEMTs. Simulations with donor traps specified at the InAlN/n^{++}GaN interface show no influence on the transfer characteristic. Our results show that the presence of acceptor traps affects the concentration of free carriers in the channel. Rapid decreases of the drain current and of the off-state current are observed with increasing acceptor trap concentration.

Acknowledgements

This work was supported by the ENIAC JU project no. 324280/2012 E2COGaN, by the grant VEGA 0866/11, by the Slovak R&D Agency grant APVV-0367-(11) and by the competence center for new materials, advanced technologies, and energy, Project No. 26240220073.

References

[1] J. Kuzmik, S. Vitanov, Ch. Dua, J.-F. Carlin, C. Ostermaier, A. Alexewicz, G. Strasser, D. Pogany, E. Gornik, N. Grandjean, S. Delage, V. Palankovski,

Buffer-related degradation aspects of single and double-heterostructure quantum well InAlN/GaN high electron mobility transistors, Jpn. J. Appl. Phys. 51 (May) (2012) 054102.
[2] A. Chini, F. Soci, M. Meneghini, G. Meneghesso, E. Zanoni, Deep levels characterization in GaN HEMTs-Part 2: experimental and numerical evaluation of self-heating effects on the extraction of traps activation energy, IEEE Trans. Electron Dev. 60 (October (10)) (2013) 3176–3182.
[3] M. Faqir, M. Bouya, N. Malbert, N. Labat, D. Carisetti, B. Lambert, G. Verzellesi, F. Fantini, Analysis of current collapse effect in AlGaN/GaN HEMT: experiments and numerical simulations, Microelectron. Reliab. 50 (August) (2010) 1520–1522.
[4] A. Sasikumar, A.R. Arehart, S. Martin-Horcajo, M.F. Romero, Y. Pei, D. Brown, F. Recht, M.A. Di Forte-Poisson, F. Calle, M.J. Tadjer, S. Keller, S.P. DenBaars, U.K. Mishra, S.A. Ringel, Direct comparison of traps in InAlN/GaN and AlGaN/GaN high electron mobility transistors using constant drain current deep level transient spectroscopy, Appl. Phys. Lett. 103 (July (3)) (2013) 033509.
[5] TCAD Sentaurus, SDevice User Guide, ver. G-2012.06, Synopsys, 2012 June.
[6] R. Wang, Y. Cai, C. Wilson, W. Tang, K.M. Lau, Kevin J. Chen, Device isolation by plasma treatment for planar integration of enhancement/depletion-mode AlGaN/GaN high electron mobility transistors, Jpn. J. Appl. Phys. 46 (4B) (2007) 2330–2333.
[7] J. Kuzmík, C. Ostermaier, G. Pozzovio, B. Basnar, W. Schrenk, J.-F. Carlin, M. Gonschorek, E. Feltin, N. Grandjean, Y. Douvry, Ch. Gaquière, J.-C. De Jaeger, K. Čičo, K. Fröhlich, J. Škriniarová, J. Kováč, G. Strasser, D. Pogany, E. Gornik, Proposal and performance analysis of normally off n^{++} GaN/InAlN/AlN/GaN HEMTs with 1-nm-thick InAlN barrier, IEEE Trans. Electron Dev. 57 (September (9)) (2010) 2144–2154.
[8] V. Palankovski, J. Kuzmik, A promising new n++GaN/InAlN/GaN HEMT concept for high-frequency applications, in: R. Garg, K. Shenai (Eds.), Gallium Nitride and Silicon Carbide Power Technologies 2, The Electrochemical Society, ECS Transactions 50 (3) (2012) 291–296, ISBN: 978-1-60768-351-3.
[9] M. Gonschorek, J.-F. Carlin, E. Feltin, M.A. Py, N. Grandjean, V. Darakchieva, B. Monemar, M. Lorenz, G. Ramm, Two-dimensional electron gas density in InxAl1-xN/AlN/GaN heterostructures ($0.03 \leq x \leq 0.23$), J. Appl. Phys. 103 (May) (2008) 093714.
[10] J. Kuzmik, InAlN/(In)GaN high electron mobility transistors: some aspects of the quantum well heterostructure proposal, Semicond. Sci. Technol. 17 (2002) 540.
[11] S. Vitanov, V. Palankovski, G. Pozzovivo, J. Kuzmik, R. Quay, Systematical study of InAlN/GaN devices by numerical simulation, in: European Workshop on Heterostructure Technology (HETECH) Book of Abstracts, Venice, 2008 November, pp. 159–160.
[12] J. Osvald, Simulation of the influence of interface states on capacitance characteristics of insulator/AlGaN/GaN heterojunctions, Phys. Stat. Sol. A 210 (March (7)) (2013) 1340–1344.